Atmos. Meas. Tech. Discuss., 5, 7067–7094, 2012
www.atmos-meas-tech-discuss.net/5/7067/2012/
doi:10.5194/amtd-5-7067-2012

Atmospheric Measurement Techniques Discussions

Development of a new JMA flask sampling and trace gas measuring system for observation on a cargo aircraft C-130H

K. Tsuboi[1], H. Matsueda[1], Y. Sawa[1], Y. Niwa[1], M. Nakamura[2], D. Kuboike[2], K. Saito[2], H. Ohmori[2], S. Iwatsubo[2], H. Nishi[2], Y. Hanamiya[2], K. Tsuji[2], and Y. Baba[2]

[1]Geochemical Research Department, Meteorological Research Institute, Tsukuba, Japan
[2]Japan Meteorological Agency, Tokyo, Japan

Received: 31 August 2012 – Accepted: 10 September 2012 – Published: 21 September 2012

Correspondence to: K. Tsuboi (ktsuboi@mri-jma.go.jp)

Published by Copernicus Publications on behalf of the European Geosciences Union.

Abstract

We developed and evaluated a flask air sampling system for atmospheric trace gas observation on a cargo C-130H aircraft, as well as an automated analysis system for the flask samples, as part of a new operational monitoring program of the Japan Meteorological Agency (JMA). Air samples were collected during each flight, between Kanagawa Prefecture (near Tokyo) and Minamitorishima (an island located nearly 2000 km southeast of Tokyo), from the air-conditioning system on the aircraft. The quality assurance test of the flask sampling air was made by specially coordinated flights at a low altitude of 1000 ft over Minamitorishima and comparing the flask values with those obtained at the surface. Based on our storage tests, the flask samples remained stable until analyses. The concentration measuring system for the flask samples has, in addition to the conventional sensors, two laser-based analyzers using wavelength-scanned cavity ring-down spectroscopy (WS-CRDS) and off-axis integrated cavity output spectroscopy (ICOS). Laboratory tests of the measuring system indicated relatively high reproducibility with overall precisions of less than 0.06 ppm for CO_2, 0.68 ppb for CH_4, 0.36 ppb for CO, and 0.03 ppb for N_2O. Inter-comparison experiments for ambient air measurements showed excellent agreements between the laser-based measurement techniques and the conventional methods currently in use. We also found that there are no significant influences of isotope effects for the laser-based analyzers.

1 Introduction

East Asia is one of the more prominent source areas of anthropogenic trace gases, and their emissions have been rapidly increasing due to the recent economic growth in Asian countries (Akimoto, 2003). For example, growth of carbon dioxide (CO_2) emissions from fossil-fuel burning and industrial processes has been accelerating in East Asia, particularly in China (Gregg et al., 2008). The CO_2 and other gaseous pollutants emitted from East Asia affect not only the regional environment over the Western North

AMTD
5, 7067–7094, 2012

Pacific (e.g. Sawa et al., 2007; Wada et al., 2011) but also the air quality over North American continent as a result of the transpacific transport (e.g. Liang et al., 2004). Thus, maintaining and expanding long-term observations of atmospheric trace gases over the Western North Pacific is important and necessary to evaluate changes in anthropogenic emissions and their influences from East Asia.

In the Western North Pacific region, long-term monitoring of CO_2 and other trace gases such as methane (CH_4) and carbon monoxide (CO) in the boundary layer has been carried out at several ground-based stations (Tohjima et al., 2002; Wada et al., 2011) and on cruise ships (Yashiro et al., 2009; Terao et al., 2011). Intensive aircraft measurement campaigns have also been carried out to examine the chemical composition of Asian continental outflows (e.g. Jacob et al., 2003, Machida et al., 2003; Sawa et al., 2004). In addition to these snapshot measurements by the aircraft campaigns, long-term observational data have been provided by measurements on commercial airliners in the free troposphere over the Western North Pacific (Nakazawa et al., 1993; Matsueda et al., 2008; Sawa et al., 2012). Model simulations of these observations showed that export of anthropogenic gases from the Asian continent to the Western Pacific through the middle and upper troposphere is particularly important for the transpacific transport (e.g. Liang et al., 2004). Thus, more systematic and long-term tropospheric measurements of trace gases by using regular aircraft observations are still needed to better understand the widespread pollution in the middle and upper troposphere over the North Pacific region.

In 2011, the Japan Meteorological Agency (JMA) started a new aircraft observation of trace gases as one of the operational atmospheric monitoring programs over the Western North Pacific. The JMA aircraft observation is made by using a cargo aircraft C-130H of the Japan Ministry of Defense (MOD) to collect flask air samples during a regular flight between the mainland of Japan and Minamitorishima once a month. In preparation for the aircraft measurement program, the JMA, in collaboration with the Meteorological Research Institute (MRI), developed a flask air sampling method and validated its reliability through laboratory experiments and preliminary test flights. In

AMTD
5, 7067–7094, 2012

this paper, we describe the sampling method employed on the C-130H aircraft, and report results of its evaluation tests.

For analyzing the C130H aircraft samples, a new automated analysis system was also developed to measure concentrations of CO_2, CH_4, CO, and nitrous oxide (N_2O). We present this analysis system and its performance. Our measuring system utilizes two laser-based instruments, because they have several key advantages such as high precision, improved stability, low maintenance, and easier operation, compared with various conventional gas chromatograph (GC) methods. The laser-based instruments have been used for in situ continuous measurements (Chen et al., 2010; Winderlich et al., 2010; Richardson et al., 2012). We report on some specific technical improvements of the laser-based instruments that went into our flask sample analysis system.

2 Sampling and analysis methods

2.1 Sampling flight

The MOD operates a routine supply flight once a month using a cargo aircraft C-130H from Atsugi base (35°27′ N, 139°27′ E) in Kanagawa Prefecture near Tokyo to a small coral island of Minamitorishima (MNM) (24°17′ N, 153°59′ E), about 2000 km southeast of Tokyo. In cooperation with the Japan Marine Self-Defense Force of the MOD, these flights enable us to regularly collect air samples over the Western North Pacific region. At MNM, the JMA operates a ground-based monitoring station to conduct long-term atmospheric measurements of CO_2, CH_4, CO and O_3 as part of the Global Atmosphere Watch programme of the World Meteorological Organization (WMO/GAW). Details of the continuous measurement system at the MNM station are reported elsewhere (Wada et al., 2007).

From June to December in 2010, preliminary observation flights using the C-130H aircraft were made to test the manual air sampling procedure on board the aircraft. In particular, specially coordinated flights at a low altitude of 1000 ft during the climb or

AMTD
5, 7067–7094, 2012

descent over MNM were carried out in order to evaluate the quality of the concentration measurements of the sampled air from the aircraft, by comparing them with the ground-based measurements obtained at the MNM station. Since February 2011, operational observations have been carried out during southbound flights to MNM which takes about 4 h at a cruising altitude of about 6 km. We collect 20 flask samples during the level flight, as well as 4 samples during the descent portion of the flight over MNM. Sampling locations are determined based on latitude, longitude and altitude from the flight navigation data of the aircraft.

2.2 Flask air sampling

Flask air sampling for the C-130H flight is manually operated by two JMA personnel on board the aircraft. Therefore, a diaphragm pump (Model N022, KNF) is modified to sample air by manual rotation. Air samples are collected from the air-conditioning system in the C-130H aircraft, similar to the procedure employed for the Boeing 747 aircraft observation (Matsueda and Inoue, 1996). Fresh air outside the aircraft is compressed by an engine and fed into the air-conditioning ducts by passing it through a pneumatic system and air cycle packs. A Teflon tube with a diameter of 1/4 in for the air sampling intake is inserted into the air-conditioning bowing nozzle upstream of the recirculation fan so that the sample air is not contaminated with the cabin air. Because the air-intake nozzle is located near the cockpit, the Teflon tube (7 m long, 1/4 in) is laid along the ceiling and extended toward the cabin, where the pump is installed in front of a passenger seat. A stainless-steel filter (60 µm mesh size) is connected to the air sample tube to remove coarse dust from the air-conditioning duct. In front of the pump, a dryer tube (35 cm long, 3/4 in) packed with CO_2-saturated magnesium perchlorate is used to reduce the water vapor in the sample air. The dried sample air is collected into a sample flask by pressurizing it to about 0.4 MPa by means of a manual pump.

We prepared new cylindrical flasks, each with an internal volume of about 1.7 l (300 mm long, 100 mm ID), which are made of titanium with a thickness of 1.2 mm to reduce the total weight. The internal surface of the flask is smoothed by electrochemical

AMTD
5, 7067–7094, 2012

polishing, and is coated with amorphous silicon with a thickness of less than 1 µm (Smith et al., 2006) to minimize the drift of trace gas concentrations in the sampled air during storage. At both ends of each flask, stainless-steel bellows valves (SS-4H, Swagelok) are attached. Furthermore, quick connectors (Swagelok QC series) are adopted to easily connect the sample inlet and vent tubes in the aircraft. Before each flight, all of the flasks are pre-treated by heating at 120 °C under a vacuum condition (1×10^{-6} Torr) to clean the internal surface. A total of 24 flasks used for each flight are divided into 4 aluminium packages, so that they can be easily placed or removed from the aircraft.

2.3 Analysis system

We developed a new automated analysis system for measuring concentrations of CO_2, CH_4, CO and N_2O in flask air samples collected from the C-130H aircraft flights. This system is comprised of spectroscopic analyzers that include laser-based instruments of a wavelength-scanned cavity ring-down spectroscopy (WS-CRDS) analyzer (Picarro, G2301) for CO_2 and CH_4 (Crosson, 2008), and an off-axis integrated cavity output spectroscopy (ICOS) analyzer (Los Gatos Research, DLT100) for N_2O and CO (Baer et al., 2002). In addition, two conventional spectroscopic sensors of a non-dispersive infrared (NDIR) analyzer (Licor, LI-7000) for CO_2 and a vacuum ultraviolet resonance fluorescence (VURF) analyzer (Aero-Laser, AL5002-AIR) for CO (Gerbig et al., 1999) are also combined. This enables us to compare the CO_2 and CO measurements between the conventional and laser-based methods.

Figure 1 shows a schematic diagram of the measuring system. The system is designed to automatically measure trace gas concentrations of 6 flask samples by a special operational program in PC. Sample flasks are connected using VCO (Swagelok) attachments at the main airflow line. For concentration calibration of the sample measurements, multi-component working standard gases are introduced by using two multi-position rotary valves (Valco) of ten ports. Before the introduction of the standard gas, a vent line is opened to exhaust any remaining gas in the pressure regulator attached

AMTD
5, 7067–7094, 2012

to the standard gas cylinder. The sample air and standard gas are passed through the cold-trap unit with two Stirling coolers (Twinbird), one at −20 °C and another one at −60 °C, to effectively remove the water vapor. The temperature of the dried sample is then raised to a room temperature by passing through a heating unit.

The main flow of the dried air sample is then divided and channeled into the four analyzers. The subsample flow rates into the analyzer cells are kept constant by mass flow controllers at 40 ml min^{-1} for the VURF and WS-CRDS, 50 ml min^{-1} for the ICOS, and 120 ml min^{-1} for the NDIR. The sample pressures in the analyzer cells are precisely maintained at 0.75 kPa for the VURF, 18.7 kPa for the WS-CRDS, 86 kPa for the ICOS, and 105 kPa for the NDIR by using auto pressure controllers. The cell pressure for the WS-CRDS analyzer is controlled by its own system, while auto pressure controllers developed in this study are used for the other three analyzers. The subsample flow is maintained for about 10 min to ensure stabilization of the analyzer responses. Their output signals from the last 3 min are used to calculate the concentrations

When we introduce the next flask sample air, the main airflow line including the cold-trap unit is evacuated by a vacuum pump for about 1 min to quickly purge the main airflow line. During this process, a purge gas with a similar trace gas composition as that of the ambient air is introduced into the analyzers at a constant flow rate by switching 2-way valves. This enables us to avoid longer drifts of the analyzer signals associated with changes in the sample flow rate and cell pressure. Since we found that such drifts largely affect the analytical precisions, the continuous air-supply system by switching from the sample or standard gas to the purge gas is essential for our discrete flask sample measurements

2.4 Standard gases

All flask concentration measurements are traceable to five multi-component working standard gases including CO_2, CH_4, CO and N_2O in purified natural air. They are filled in 48-l aluminum high-pressure cylinders, which are prepared using a volumetric method by a gas company (Japan Fine Products Corp. (JFP), Japan). The drifts of the

AMTD
5, 7067–7094, 2012

working standards are regularly investigated by comparing with the primary standard gases maintained in a JMA calibration system. In this calibration system, CO_2 is analyzed by a non-dispersive infra-red gas analyzer (NDIR; Horiba, VA510R), while other trace gases are analyzed by gas chromatographs (GCs) equipped with a flame ionization detector (GC/FID: Shimadzu, GC14B) for CH_4, a reduction gas detector (GC/HgO: RoundScience, TRA-1) for CO, and an electron capture detector (GC/ECD: Shimadzu GC-2014) for N_2O, respectively. Analytical precisions for repetitive measurements are less than 0.02 ppm for CO_2, 2 ppb for CH_4, 1 ppb for CO, and 0.3 ppb for N_2O.

All mixing ratios in this paper are reported in parts per million (ppm), parts per billion (ppb) by mole fraction in dry air traceable to the JMA primary standards. Their standards are calibrated based on the World Meteorological Organization (WMO) mole fraction scales for CO_2 (Zhao and Tans, 2006), CH_4 (Dlugokencky et al., 2005), CO (Novelli et al., 2003), and N_2O (Hall et al., 2007). The WMO scales are propagated from the Global Monitoring Division (GMD) of the National Oceanic and Atmospheric Administration (NOAA) Earth System Research Laboratory, which serves as the central calibration laboratory.

3 Results and discussions

3.1 Quality of flask sample air

For the flask sampling, we have collected sample air passing through the air-conditioning system of the C-130H aircraft, similar to the technique employed on Boeing 747 (Matsueda et al., 1996; Machida et al., 2008). However, a quality-assurance test of the sample air under actual flight condition of C-130H aircraft had not been performed. Therefore, in 2010, specially coordinated flights using C-130H were made at a very low altitude of 1000 ft over MNM, and the aircraft measurements were compared with the JMA ground-based measurements at the MNM station. This exercise

AMTD
5, 7067–7094, 2012

was suitable around MNM, because the influence of the local sources and sinks on the MNM island is negligible on the trace gas observations there (Wada et al., 2007).

During each low-level flight at 1000 ft, 4 air samples were collected in stainless steel flasks, and were then returned to the MRI for analysis of CO_2, CH_4 and CO concentrations using a MRI analysis system (Matsueda and Inoue, 1996; Matsueda et al., 1998). In total, 7 flights were made each month during June–December in 2010. Because of the fact the MRI standard gas scales and analytical instruments are different from those at the JMA, all the flask samples collected from the aircraft and the surface station were analyzed at the MRI, so that we could compare surface and aircraft concentration values with minimal systematic bias and uncertainty.

Figure 2 shows the temporal variations of measured concentrations for CO_2, CH_4 and CO obtained from the aircraft during the 7 experimental flights, and are compared to the hourly surface mean data (at 20 m height) obtained at the JMA monitoring station. Each aircraft value is an average of four flask measurements. The four measurements nearly agree to within the analytical precisions. Both the aircraft and surface data correlate reasonably well in showing distinct seasonal variations, as well as short-term variations. The mean differences of 24 individual measurements (aircraft data – ground-based data) are estimated to be +0.2 ppm with a SD of 0.3 ppm for CO_2, −0.7 ppb with a SD of 3.3 ppb for CH_4, and +2.4 ppb with a SD of 4.1 ppb for CO. These differences are not viewed as significant, given the uncertainties of the sampling and analytical errors, not to mention the slight difference in the sampling height. These results indicate that CO_2, CH_4 and CO concentrations in the sampled air are not changed by passing it through the air-conditioning system of the C-130H aircraft, confirming the reliability of the overall flask sampling procedure on board the C-130H aircraft for high-precision trace gas measurements.

3.2 Storage test for sample flask

After sampling, it takes about 2–3 days for flasks to arrive at the JMA laboratory for concentration analysis. To estimate the magnitude of the concentration drift of each

AMTD
5, 7067–7094, 2012

trace gas in the flask during the transport, storage experiments using dry natural air were performed. Each flask was preconditioned by heating it at 120 °C under pressure of about 1×10^{-6} Torr for 12 h. It has been shown by Murayama et al. (2003) that such treatment is effective in minimizing the CO_2 drift in flask samples. After the preconditioning, dry natural air was pumped into the flask to a pressure of 2–3 atmospheres and was immediately analyzed for CO_2, CH_4 and CO concentrations. The flasks were then kept at room temperature for 2–10 days, and were re-analyzed to calculate the drift. These analyses were performed using the MRI measuring system.

From the storage experiments, we estimated mean linear drifts of $+0.012\,\mathrm{ppm\,day^{-1}}$ with a standard deviation (SD) of $0.017\,\mathrm{ppm\,day^{-1}}$ ($n = 48$) for CO_2, $+0.05\,\mathrm{ppb\,day^{-1}}$ with a SD of $0.27\,\mathrm{ppb\,day^{-1}}$ ($n = 28$) for CH_4, and $+0.19\,\mathrm{ppb\,day^{-1}}$ with a SD of $0.44\,\mathrm{ppb\,day^{-1}}$ ($n = 28$) for CO. These results indicated no significant changes in the concentrations of CO_2, CH_4 and CO during the 2–3 day transport of the flasks between the time of collection and analysis. It has been reported that CO concentration in a metal flask increases at a rate of about $0.6\,\mathrm{ppb\,day^{-1}}$ (e.g. Matsueda et al., 1998; Machida et al., 2008), but the precondition process we carried out to prepare the flasks helped to minimize this problem. Thus, all of the flasks are heated and evacuated before aircraft sampling.

3.3 Analysis and its precision

In our measuring system, 6 flask samples can be automatically analyzed together with the working standard gases. The data from the four analyzers, as well as from pressure and temperature sensors, are collected at an interval of 2 s. Figure 3 shows an example of the temporal variations of CO_2, CH_4, CO, N_2O, H_2O and sample pressure when 6 flasks with natural air were analyzed. To calibrate the measurements of the sample air, 5 working standard gases are introduced before and after 3 successive flask sample analyses. This sequence was found to be optimal for high-precision calibration of the flask sample measurements based on various experimental tests. Each analysis

AMTD
5, 7067–7094, 2012

run for one flask sample or one standard gas takes about 12 min, consisting of 2 min for evacuation and sample purge of the main flow line, and the remaining 10 min. for sample flow to the analyzers. For the 10-min sample flow, the air pressures of the flask samples decrease from about 300 kPa to 150 kPa (Fig. 3e), but all the output signals for CO_2, CH_4, CO, N_2O appear to be relatively constant, showing invariance of the analyzers with sample pressure (Fig. 3a, b, c, d). That is, when 1-min averaged analyzer signals are calculated, we find no significant fluctuations for the last 5 min of the 10-min sample flow. The water vapor (H_2O) signals from the WS-CRDS analyzer show no significant difference between the sample air and dry standard gases with their H_2O content of less than 0.005 % (Fig. 3f). We have confirmed by more experimental tests that the H_2O content in a wetter air sample is reduced to at least less than 0.01 %. These results indicate no significant influence of H_2O content on the analyses of the flask samples.

To evaluate the overall analytical precisions of our instrument, one multi-component standard gas with known concentrations of the trace gases was filled into 6 sample flasks and then analyzed by the same analysis procedural sequence described above. Results from this experiment are summarized in Table 1. Measurements from the WS-CRDS and ICOS analyzers showed high reproducibility for all the trace gas analyses with SDs of less than 0.06 ppm for CO_2, 0.68 ppb for CH_4, 0.36 ppb for CO, and 0.03 ppb for N_2O. These values are comparable or better than those obtained from the conventional methods at the WMO Central Calibration Laboratory of NOAA/GMD (Novelli et al., 2003; Dlugokencky et al., 2005; Zhao and Tans, 2006; Hall et al., 2007). In addition, the measured concentrations of all the trace gases agree well with those assigned by the JMA calibration system.

3.4 Calibration curve

Since the response linearity of the NDIR and VURF analyzers had been well examined, we report here only the calibration curves for the new laser-based analyzers of the WS-CRDS and ICOS instrument. Figure 4 plots the output signals versus the

AMTD
5, 7067–7094, 2012

concentrations for CO_2 and CH_4 from the WS-CRDS analyzer, and N_2O and CO from the ICOS analyzer. They are the analysis results of the five working standard gases. The concentrations were determined by using the JMA calibration system based on the WMO mole fraction scales. It is noted that the CO values are given by the re-calibration from the VURF analyses, because the GC/HgO method of the JMA calibration system has larger analytical errors due to the non-linearity response of the HgO detector (Novelli et al., 2003).

As shown in Fig. 4, residuals between the linear fit curves and measured values are calculated to be less than 0.05 ppm for CO_2, less than 0.7 ppb for CH_4, less than 0.8 ppb for CO, and less than 0.3 ppb for N_2O. These deviations from the linear calibration curves are not significant considering the analytical uncertainties associated with both the JMA calibration and our measurement system. These results indicate not only high linearity of the responses for both WS-CRDS and ICOS but also internal consistency of the assigned concentrations for the 5 working standard gases. Thus, we feel confident that our analysis system with the laser-based analyzers makes high-precision measurements that are accurately traceable to the WMO mole fraction scales.

3.5 Isotope effect

The laser-based analyzers of the WS-CRDS for CO_2 and CH_4 and ICOS for CO and N_2O potentially have some measurement errors due to their isotope effects (e.g. Chen et al., 2010). In our measuring system, the isotope effect results mainly from the differences in isotopic composition between a natural atmospheric sample and an artificial working standard gas. Thus, we evaluated the isotope effects using a similar method reported by Chen et al. (2010). Direct measurements of the isotopic ratios of our working standard gases were not available, but we were able to obtain their approximate values because of the known fossil fuel origin of the parent gases used in the working standards, as discussed below. All isotopic ratios in this study are expressed as delta (δ) values relative to the ratio of the reference materials of the Vienna Pee Dee Belemnite (VPDB) and Vienna Standard Mean Ocean Water (VSMOW) in this study.

AMTD
5, 7067–7094, 2012

To calculate the isotope effect of the WS-CRDS system for CO_2, we used −27 ‰ for $\delta^{13}C$ and +18 ‰ for $\delta^{18}O$ as CO_2 in our working standard gases. These isotopic ratios were derived from previous measurements of several CO_2 standard gas cylinders filled by the same gas company JFP (former Nippon Sanso Corp., Japan) during 1993–2004. On the other hand, the $\delta^{13}C$ and $\delta^{18}O$ values of ambient CO_2 were assigned −8 ‰ (Nakazawa et al., 1993) and +42 ‰ (Allison and Francey, 2007), respectively. Using these values, the isotope effect was estimated to be about 0.11–0.13 ppm (CO_2 of 360–420 ppm), which is slightly smaller than a previous estimate of 0.14–0.16 ppm (Chen et al., 2010). When we used −32.43 ‰ for $\delta^{13}C$ and +11.7 ‰ for $\delta^{18}O$ for CO_2 standard gas from the JFP (Tohjima et al., 2009), the isotope effect was also calculated to be about 0.14–0.16 ppm. These results indicate that the isotope effect associated with the CO_2 measurements made by the WS-CRDS analyzer ranges from about 0.11 to 0.16 ppm.

For calculating the isotope effect associated with the WS-CRDS analyzer for CH_4, we used the representative values of fossil fuel CH_4 with −40 ‰ for $\delta^{13}C$ and −175 ‰ for δD for the working standard gases (Snover et al., 2000). These isotopic values are similar to those obtained by direct measurements of several CH_4 standard gases obtained from the JFP (T. Umezawa, personal communication, 2011). On the other hand, the isotopic ratios of atmospheric CH_4 are around −47 ‰ for $\delta^{13}C$ and −95 ‰ for δD observed in the Western North Pacific region (Umezawa et al., 2009). Using these values, the isotope effect was estimated to be about −0.05 to −0.06 ppb (CH_4 of 1700–2200 ppb), which is much smaller than the analytical precision for CH_4 concentration. Thus, the isotope effect of the WS-CRDS analyzer for CH_4 can be ignored.

To calculate the isotope effect of the ICOS analyzer for N_2O, we used the values −2 to −3 ‰ for $\delta^{15}N$ and +25 to +26 ‰ for $\delta^{18}O$, which are based on the measurements of several N_2O standard gases obtained from the JFP (K. Ishijima, personal communication, 2011). Meanwhile, recent isotopic ratios of atmospheric N_2O are around +7 ‰ for $\delta^{15}N$ and +45 ‰ for $\delta^{18}O$ obtained from several ice core firn air analyses (Ishijima et al., 2007). Using these values, the isotope effect was estimated to be about 0.032–

AMTD
5, 7067–7094, 2012

0.035 ppb (N_2O of 310–340 ppb), which is about the same as the analytical precision for N_2O concentration measurements. This result indicates no significant influence of the isotope effect on the N_2O measurement by the ICOS analyzer.

Lastly, to calculate the isotope effect of the ICOS analyzer for CO, we have a wide range of values, from −22 to −50 ‰ for $\delta^{13}C$ and +10 to +22 ‰ for $\delta^{18}O$ that can be used for CO in a working standard gas, assuming fossil fuel origin such as natural gases, gasoline and diesel (Kato et al., 1999; Coplen et al., 2002). On the other hand, the isotopic ratios of atmospheric CO have been measured to be around −27 ‰ for $\delta^{13}C$ and +10 ‰ for $\delta^{18}O$ over Germany (Kato et al., 1999). Using these values, the isotope effect was estimated to be less than ±0.1 ppb (CO of 0–300 ppb), again indicating no significant influence of the isotope effect on the CO measurement by the ICOS analyzer.

3.6 Inter-comparison of different measuring techniques

Laser-based spectroscopic analyses are possibly biased not only by the isotope effect but also by the pressure-broadening effect resulting from the difference in the composition between a standard gas and ambient air. The pressure-broadening effect is caused mainly by the differences in the water vapor content and the composition of the matrix gas (N_2, O_2, Ar) (Chen et al., 2010). Although the water vapor influence associated with the pressure-broadening and dilution effect is minimized by the drying procedure in our measuring system, the effect due to the matrix gas composition is estimated to have a small influence (Nara et al., 2012). Because it is difficult to quantify all of these individual effects, inter-comparisons among different measuring techniques were made based on the direct measured values of ambient air to evaluate the whole instrumental bias.

In our measuring system, the CO_2 concentration of our flask air samples is simultaneously measured by the WS-CRDS and NDIR analyzers, to compare their relative values. Figure 5a shows a frequency distribution of the differences in the measured CO_2 concentration between the WS-CRDS and the NDIR analyzers for the flask air

AMTD
5, 7067–7094, 2012

samples collected by the C-130H aircraft flights from February to August in 2011. The mean difference (WS-CRDS minus NDIR) was +0.027 ppm with a SD of 0.066 ppm when we compared 213 air sample analyses. We found no systematic difference as a function of CO_2 concentration. These results show good agreement between the two different measuring techniques for CO_2. This strongly suggests that the isotope effect in the WS-CRDS analyzer is comparable to the similar effect in the NDIR analyzer caused by its optical band-pass filter. Indeed, to evaluate the NDIR isotope effect, we measured the optical property of the filter by using a $^{13}CO_2$-in-air mixture, following the method reported by Tohjima et al. (2009). From this experiment, the isotope effect of our NDIR was estimated to be 0.075–0.087 ppm (CO_2 of 360–420 ppm), which is similar to that of the WS-CRDS analyzer (0.11–0.16 ppm). This indicates that the isotope effects between the two analyzers are comparable to each other considering several uncertainties in the estimation.

We also performed an inter-comparison of CO measured simultaneously by the ICOS and the VURF analyzers. Figure 5b shows a frequency distribution of the differences in the measured CO concentration between the VURF and the ICOS analyzers for 128 flask air samples collected by the C-130H aircraft flights from April to August in 2011. The mean difference (ICOS minus VURF) was +0.12 ppb with a SD of 0.25 ppb, indicating an excellent agreement of CO data between the two analyzers. This agreement is due primarily to a very small isotope effect of about 0.1 ppb for the laser-based ICOS analyzer, as described in Sect. 3.5. This is consistent with study by Zellweger et al. (2009) who found a good agreement between the VURF and GC/HgO methods from their field inter-comparison tests. That is, there does not appear to be any significant bias in the new CO measuring technique using the ICOS analyzer, compared with the conventional GC/HgO and/or VURF methods commonly employed for background atmospheric CO observations (e.g. Novelli et al., 2003).

As for CH_4 and N_2O, only the WS-CRDS and ICOS laser-based analyzers are used in our measuring system. Thus, in order to assess the fidelity of these measurement systems, we carried out an inter-comparison exercise in which flask air samples were

AMTD
5, 7067–7094, 2012

analyzed by the GC analysis system (GC/FID for CH_4 and GC/ECD for N_2O) in the JMA calibration laboratory after they were finished with the laser-based analyzers. The flask samples collected by the C-130H aircraft flights from February to August in 2011 were used for the comparison. Figures 5c and d show frequencies of the differences in CH_4 between the WS-CRDS and GC/FID analyzers, and in N_2O between the ICOS and GC/ECD analyzers, respectively. The mean difference for CH_4 (WS-CRDS minus GC/FID) was +0.70 ppb with a SD of 2.27 ppb ($n = 74$), while the mean difference for N_2O (ICOS minus GC/ECD) was +0.15 ppb with a SD of 1.11 ppb ($n = 103$). These small differences in the mean values indicate a good agreement between the laser-based technique and the conventional GC method for both CH_4 and N_2O, although their SD values are somewhat large due to analytical errors of the GC methods. This is consistent with very small isotope effects of less than 0.1 ppb in the CH_4 and N_2O measurements by both the WS-CRDS and ICOS analyzers, as stated in Sect. 3.5. Thus, we conclude that there is no significant bias for measuring CH_4 and N_2O concentrations by the new laser-based instruments.

4 Conclusions

To set up a flask air sampling system by using a cargo C-130H aircraft, we examined its reliability for analyses of atmospheric trace gas concentrations. The quality assurance test of the air-conditioning air used for the flask sampling was made by specially coordinated flights at a low altitude of 1000 ft over Minamitorishima. It was demonstrated that the overall procedure of our flask sampling method in the aircraft is suitable for appropriately collecting air samples without contamination and modification of trace gases concentrations. In addition, new flasks, with internal surfaces coated with silicon, were evaluated by the storage tests to ensure the stability of the trace gases. The average 2–3 day storage between the time of collection and analysis did not produce any noticeable drift in the trace gas concentration.

AMTD
5, 7067–7094, 2012

We also developed an automated measuring system for flask samples, comprising of Stirling coolers for sample drying, 5 working standard gases for calibration, and 4 analyzers to measure CO_2, CH_4, CO, and N_2O concentrations. This system utilizes not only conventional sensors but also new laser-based analyzers using WS-CRDS and ICOS sensors. The laboratory experiment using 6 flasks filled with a standard gas showed high reproducibility of our laser-based analyzers for all the trace gas. Their isotope effects were estimated to be negligible except for the CO_2 measurement. We demonstrated no systematic differences in the aircraft sample measurements between the new laser-based spectroscopies and the conventional methods. In this study, the laser-based instruments were employed first for discrete flask samples analyses to achieve high-precision measurements accurately traceable to the WMO mole fraction scales. At present, a sufficiently large amount of sample air is conservatively used at the first application step, but the measuring system and the analytical condition could be improved to utilize to use a smaller amount of sample air. Thus, our measuring system has the potential to be widely used for flask sample analyses based on the laser-based instruments.

Current attempts to infer anthropogenic emissions of trace gases in East Asia by various top-down inverse methods are limited by the sparseness of the available observation data. In particular, aircraft measurements above the planetary boundary layer are useful for the inversion approaches to strongly constrain and reduce larger uncertainties of flux estimates (e.g. Stephens et al., 2007; Niwa et al., 2012). Thus, the C-130H aircraft observation could provide a useful dataset with sufficiently high quality over the Western North Pacific to better understand the trace gas emissions in East Asia and their long-range transports through the free troposphere. The dataset is posted on the WMO World Data Centre for Greenhouse Gases (WMO/WGCGG, http://ds.data.jma.go.jp/gmd/wdcgg/wdcgg.html) operated by JMA in Tokyo.

Acknowledgements. The authors gratefully acknowledge many staffs of Japan Ministry of Defense for supporting the aircraft observation. The authors would like to thank A. Kudo (JANS Corp. Japan) for his skillful improvement in the design and manufacturing of automated

AMTD
5, 7067–7094, 2012

measuring system, and S. Murayama (National Institute of Advanced Industrial Technology, AIST), and T. Kitao (KANSO Corp. Japan) for helpful assistance of sample flask treatment and testing. We thank Y. Tohjima (National Institute for Environmental Studies, NIES), and T. Machida (NIES) for helpful discussions and supporting experiment of NDIR isotope effect. We are grateful to K. Ishijima (Japan Agency for Marine-Earth Science and Technology), and T. Umezawa (Max Planck Institute for Chemistry) for providing valuable information of isotopic ratios of standard gases. We also thank K. Higuchi (York University) for his comments on the manuscript.

References

Akimoto, H.: Global air quality and pollution, Science, 302, 1716–1719, doi:10.1126/science.1092666, 2003.

Allison, C. E. and Francey, R. J.: Verifying Southern Hemisphere trends in atmospheric carbon dioxide stable isotopes, J. Geophys. Res., 112, D21304, doi:10.1029/2006JD007345, 2007.

Baer, D. S., Paul, J. B., Gupta, M., and O'Keefe, A.: Sensitive absorption measurements in the near-infrared region using off-axis integrated-cavity-output spectroscopy, Appl. Phys. B, 75, 261–265, doi:10.1007/s00340-002-0971-z, 2002.

Chen, H., Winderlich, J., Gerbig, C., Hoefer, A., Rella, C. W., Crosson, E. R., Van Pelt, A. D., Steinbach, J., Kolle, O., Beck, V., Daube, B. C., Gottlieb, E. W., Chow, V. Y., Santoni, G. W., and Wofsy, S. C.: High-accuracy continuous airborne measurements of greenhouse gases (CO_2 and CH_4) using the cavity ring-down spectroscopy (CRDS) technique, Atmos. Meas. Tech., 3, 375–386, doi:10.5194/amt-3-375-2010, 2010.

Coplen, T. B., Böhlke, J. K., De Bièvre, P., Ding, T., Holden, N. E., Hopple, J. A., Krouse, H. R., Lamberty, A., Peiser, H. S., Revesz, K., Rieder, S. E., Rosman, K. J. R., Roth, E., Taylor, P. D. P., Vocke, R. D., and Xiao, Y. K.: Isotope-abundance variations of selected elements (IUPAC Technical Report), Pure Appl. Chem., 74, 1987–2017, 2002.

Crosson, E. R.: A cavity ring-down analyzer for measuring atmospheric levels of methane, carbon dioxide, and water vapor, Appl. Phys. B, 92, 403–408, doi:10.1007/s00340-008-3135-y, 2008.

Dlugokencky, E. J., Myers, R. C., Lang, P. M., Masarie, K. A., Crotwell, A. M., Thoning, K. W., Hall, B. D., Elkins, J. W., and Steele, L. P.: Conversion of NOAA atmospheric dry air CH_4

AMTD
5, 7067–7094, 2012

mole fractions to a gravimetrically prepared standard scale, J. Geophys. Res., 110, D18306, doi:10.1029/2005JD006035, 2005.
Gerbig, C., Smitgen, S., Kley, D., Volz-Thomas, A., Dewey, K., and Haaks, D.: An improved fast-response vacuum-UV resonance fluorescence CO instrument, J. Geophys. Res., 104, 1699–1704, doi:10.1029/1998JD100031, 1999.
Gregg, J. S., Andres, R. J., and Marland, G.: China: emissions pattern of the world leader in CO_2 emissions from fossil consumption and cement production, Geophys. Res. Lett., 35, L08806, doi:10.1029/2007GL032887, 2008.
Hall, B. D., Dutton, G. S., and Elkins, J. W.: The NOAA nitrous oxide standard scale for atmospheric observations, J. Geophys., Res., 112, D09305, doi:10.1029/2006JD007954, 2007.
Ishijima, K., Sugawara, S., Kawamura, K., Hashida, G., Morimoto, S., Murayama, S., Aoki, S., and Nakazawa, T.: Temporal variations of the atmospheric nitrous oxide concentration and its δ^{15}N and δ^{18}O for the latter half of the 20th century reconstructed from firn air analyses, J. Geophys. Res., 112, D03305, doi:10.1029/2006JD007208, 2007.
Jacob, D. J., Crawford, J. H., Kleb, M. M., Connors, V. S., Bendura, R. J., Raper, J. L., Sachse, G. W., Gille, J. C., Emmons, L., and Heald, C. L.: Transport and chemical evolution over the Pacific (TRACE-P) aircraft mission: design, execution, and first results, J. Geophys. Res., 108, 9000, doi:10.1029/2002JD003276, 2003.
Kato, S., Akimoto, H., Bräunlich, M., Röckmann, T., and Brenninkmeijer, C. A. M.: Measurements of stable carbon and oxygen isotopic compositions of CO in automobile exhausts and ambient air from semi-urban Mainz, Germany, Geochem. J., 33, 73–77, 1999.
Liang, Q., Jaeglé, L., Jaffe, D. A., Weiss-Penzias, P., Heckman, A., and Snow, J. A.: Long-range transport of Asian pollution to the Northeast Pacific: seasonal variations and transport pathways of carbon monoxide, J. Geophys., Res., 109, D23S07, doi:10.1029/2003JD004402, 2004.
Machida, T., Kita, K., Kondo, Y., Blake, D., Kawakami, S., Inoue, G., and Ogawa, T.: Vertical and meridional distributions of the atmospheric CO_2 mixing ratio between northern midlatitudes and southern subtropics, J. Geophys. Res., 108, 8401, doi:10.1029/2001JD000910, 2003.
Machida, T., Matsueda, H., Sawa, Y., Nakagawa, Y., Hirotani, K., Kondo, N., Goto, K., Nakazawa, T., Ishikawa, K., and Ogawa, T.: Worldwide measurements of atmospheric CO_2 and other trace gas species using commercial airlines, J. Atmos. Ocean. Tech., 25, 1744–1754, doi:10.1175/2008JTECHA1082.1, 2008.

AMTD
5, 7067–7094, 2012

Matsueda, H. and Inoue, H. Y.: Measurements of atmospheric CO_2 and CH_4 using a commercial airliner from 1993 to 1994, Atmos. Environ., 30, 1647–1655, doi:10.1016/1352-2310(95)00374-6, 1996.

Matsueda, H., Inoue, H. Y., Sawa, Y., Tsutsumi, Y., and Ishii, M.: Carbon monoxide in the upper troposphere over the Western Pacific between 1993 and 1996, J. Geophys. Res., 103, 19093–19110, doi:10.1029/98JD01598, 1998.

Matsueda, H., Machida, T., Sawa, Y., Nakagawa, Y., Hirotani, K., Ikeda, H., Kondo, N., and Goto, K.: Evaluation of atmospheric CO_2 measurements from new flask air sampling of JAL airliner observations, Pap. Meteorol. Geophys., 59, 1–17, doi:10.2467/mripapers.59.1, 2008.

Murayama, S., Harada, K., Gotoh, K., Kitao, T., Watai, T., and Yamamoto, S.: On large variations in atmospheric CO_2 concentration observed over the Central and Western Pacific Ocean, J. Geophys. Res., 108, 4243, doi:10.1029/2002JD002729, 2003.

Nakazawa, T., Morimoto, S., Aoki, S., and Tanaka, M.: Time and space variations of the carbon isotopic ratio of tropospheric carbon dioxide over Japan, Tellus B, 45, 258–274, doi:10.1034/j.1600-0889.1993.t01-2-00004.x, 1993.

Nara, H., Tanimoto, H., Tohjima, Y., Mukai, H., Nojiri, Y., Katsumata, K., and Rella, C.: Evaluation of factors affecting accurate measurements of atmospheric CO_2 and CH_4 by wavelength-scanned cavity ring-down spectroscopy, Atmos. Meas. Tech. Discuss., 5, 5009–5041, doi:10.5194/amtd-5-5009-2012, 2012.

Niwa, Y., Machida, T., Sawa, Y., Matsueda, H., Schuck, T. J., Brenninkmeijer, C. A. M., Imasu, R., and Satoh, M.: Imposing strong constraints on tropical terrestrial CO_2 fluxes using passenger aircraft based measurements, J. Geophys. Res., 117, D11303, doi:10.1029/2012JD017474, 2012.

Novelli, P. C., Masarie, K. A., Lang, P. M., Hall, B. D., Myers, R. C., and Elkins, J. W.: Reanalysis of tropospheric CO trends: effects of the 1997–1998 wildfires, J. Geophys. Res., 108, 4464, doi:10.1029/2002JD003031, 2003.

Richardson, S. J., Miles, N. L., Davis, K. J., Crosson, E. R., Rella, C. W., and Andrews, A. E.: Field testing of cavity ring-down spectroscopy analyzers measuring carbon dioxide and water vapor, J. Atmos. Ocean. Tech., 29, 397–406, doi:10.1175/JTECH-D-11-00063.1, 2012.

Sawa, Y., Matsueda, H., Makino, Y., Inoue, H. Y., Murayama, S., Hirota, M., Tsutsumi, Y., Zaizen, Y., Ikegami, M., and Okada, K.: Aircraft observation of CO_2, CO, O_3 and H_2 over the North Pacific during PACE-7 campaign, Tellus B, 56, 2–20, doi:10.1111/j.1600-0889.2004.00088.x, 2004.

AMTD
5, 7067–7094, 2012

Sawa, Y., Tanimoto, H., Yonemura, S., Matsueda, M., Mukai, H., Wada, A., Taguchi, S., Hayasaka, T., Tsuruta, H., Tohjima, Y., Mukai, H., Kikuchi, N., Katagiri, S., and Tsuboi, K.: Carbon monoxide for widespread pollution events observed over the Western North Pacific during EAREX campaign 2005, J. Geophys. Res., 112, D22S26, doi:10.1029/2006JD008055, 2007.

Sawa, Y., Machida, T., and Matsueda, H.: Aircraft observations of the seasonal variation in the transport of CO_2 in the upper atmosphere, J. Geophys. Res., 117, D05305, doi:10.1029/2011JD016933, 2012.

Smith, A. D., Barone, G. A., Higgins, M. E., Kendall, B. R. F., and Lavrich, D. J.: Method for chemical vapor deposition of silicon on to substrates for use in corrosive and vacuum environments, United States Patent No. 7, 070, 833 B2, 2006.

Snover, A. K., Quay, P. D., and Hao, W. M.: The D/H content methane emitted from biomass burning, Global Biogeochem. Cy., 14, 11–24, doi:10.1029/1999GB900075, 2000.

Stephens, B. B., Gurney, K. R., Tans, P. P., Sweeney, C., Peters, W., Bruhwiler, L. M., Ciais, P., Ramonet, M., Bousquet, P., Nakazawa, T., Aoki, S., Machida, T., Inoue, G., Vinnichenko, N., Lloyd, J., Jordan, A., Heimann, M., Shibistova, O. B., Langenfelds, R. L., Steele, L. P., Francey, R. J., and Denning, A. S.: Weak northern and strong tropical land carbon uptake from vertical profiles of atmospheric CO_2, Science, 316, 1732–1735, doi:10.1126/science.1137004, 2007.

Terao, Y., Mukai, H., Nojiri, Y., Machida, T., Tohjima, Y., Saeki, T., and Maksyutov, S.: Interannual variability and trends in atmospheric methane over the Western Pacific from 1994 to 2010, J. Geophys. Res., 116, D14303, doi:10.1029/2010JD015467, 2011.

Tohjima, Y., Machida, T., Utiyama, M., Katsumata, M., Fujimura, Y., and Maksyutov, S.: Analysis and presentation of in situ atmospheric methane measurements from Cape Ochi-ishi and Hateruma Island, J. Geophys. Res., 107, 4148, doi:10.1029/2001JD001003, 2002.

Tohjima, Y., Katsumata, K., Morino, I., Mukai, H., Machida, T., Akama, I., Amari, T., and Tsunogai, U.: Theoretical and experimental evaluation of the isotope effect of NDIR analyzer on atmospheric CO_2 measurement, J. Geophys. Res., 114, D13302, doi:10.1029/2009JD011734, 2009.

Umezawa, T., Aoki, S., Nakazawa, T., and Morimoto, S.: A high-precision measurement system for carbon and hydrogen isotopic ratios of atmospheric methane and its application to air samples collected in the Western Pacific region, J. Meteorol. Soc. Jpn., 87, 365–379, doi:10.2151/jmsj.87.365, 2009.

AMTD
5, 7067–7094, 2012

Wada, A., Sawa, Y., Matsueda, H., Taguchi, S., Murayama, S., Okubo, S., and Tsutsumi, Y.: Influence of continental air mass transport on atmospheric CO_2 in the Western North Pacific, J. Geophys. Res., 112, D07311, doi:10.1029/2006JD007552, 2007.

Wada, A., Matsueda, H., Sawa, Y., Tsuboi, K., and Okubo, S.: Seasonal variation of enhancement ratios of trace gases observed over 10 years in the Western North Pacific, Atmos. Environ., 45, 2129–2137, doi:10.1016/j.atmosenv.2011.01.043, 2011.

Winderlich, J., Chen, H., Gerbig, C., Seifert, T., Kolle, O., Lavrič, J. V., Kaiser, C., Höfer, A., and Heimann, M.: Continuous low-maintenance CO_2/CH_4/H_2O measurements at the Zotino Tall Tower Observatory (ZOTTO) in Central Siberia, Atmos. Meas. Tech., 3, 1113–1128, doi:10.5194/amt-3-1113-2010, 2010.

Yashiro, H., Sugawara, S., Sudo, K., Aoki, S., and Nakazawa, T.: Temporal and spatial variations of carbon monoxide over the western part of the Pacific Ocean, J. Geophys. Res., 114, D08305, doi:10.1029/2008JD010876, 2009.

Zellweger, C., Hüglin, C., Klausen, J., Steinbacher, M., Vollmer, M., and Buchmann, B.: Intercomparison of four different carbon monoxide measurement techniques and evaluation of the long-term carbon monoxide time series of Jungfraujoch, Atmos. Chem. Phys., 9, 3491–3503, doi:10.5194/acp-9-3491-2009, 2009.

Zhao, C. L. and Tans, P. P.: Estimating uncertainty of the WMO mole fraction scale for carbon dioxide in air, J. Geophys. Res., 111, D08S09, doi:10.1029/2005JD006003, 2006.

AMTD
5, 7067–7094, 2012

Table 1. Results of repetitive measurements for CO_2, CH_4, CO and N_2O in a multi-component standard gas filled into 6 flasks.

Trace gas	CO_2	CO_2	CH_4	CO	CO	N_2O
Analyzer	NDIR	WS-CRDS	WS-CRDS	VURF	ICOS	ICOS
Unit	(ppm)	(ppm)	(ppb)	(ppb)	(ppb)	(ppb)
Measured (A)[a]	387.16	387.23	1779.2	101.7	101.6	314.0
SD	0.05	0.06	0.68	0.36	0.34	0.03
Assigned (B)[b]	387.17	387.14	1778.2	101.2	101.0	314.0
Difference (A) – (B)	−0.01	0.09	0.99	0.49	0.58	−0.01

[a] The measured value is an average of the 6 measurements ($n = 6$) from the measuring system developed in this study.
[b] The assigned value is derived from the calibration system using conventional methods.

AMTD
5, 7067–7094, 2012

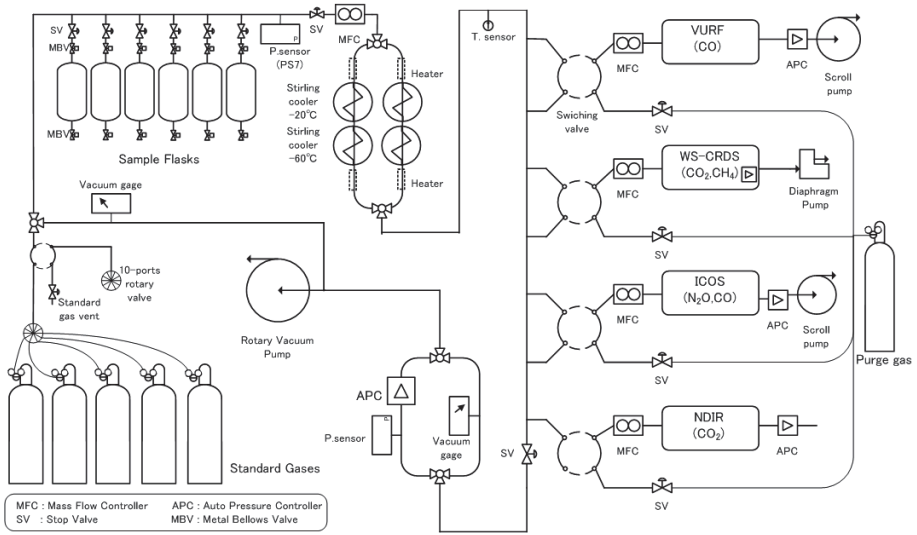

Fig. 1. Schematic diagram of the automated measuring system for flask air samples. Details of the air flow and measuring procedure are described in the text.

AMTD
5, 7067–7094, 2012

Development of a new JMA flask sampling

K. Tsuboi et al.

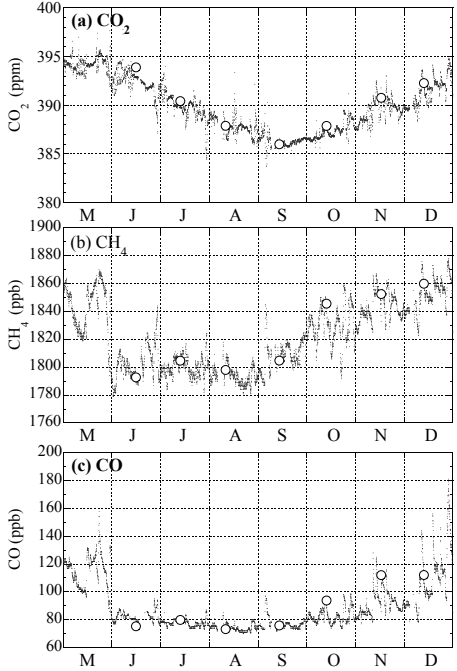

Fig. 2. Temporal variations of CO_2 **(a)**, CH_4 **(b)**, and CO **(c)** concentrations over Minamitorishima during May–December in 2010. The open circles and the solid dots represent aircraft measurements at 1000 ft (average of 4 flask samples) and hourly-averaged data from the ground-based station, respectively.

AMTD
5, 7067–7094, 2012

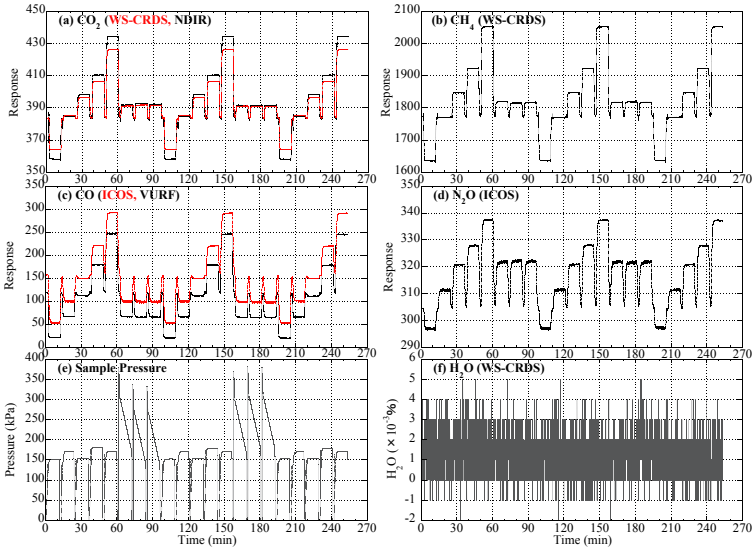

Fig. 3. An example of the response time-series of CO_2 **(a)** for the NDIR and WS-CRDS analyzers, CH_4 **(b)** for the WS-CRDS analyzer, CO **(c)** for the VURF and ICOS analyzers, N_2O **(d)** for the ICOS analyzers, sample pressure **(e)** for the pressure sensor PS-7, and H_2O **(f)** for the WS-CRDS analyzer from the experimental analyses of 6 flask air samples together with 5 working standard gases. Details of the analytical sequence and procedure are described in the text.

AMTD
5, 7067–7094, 2012

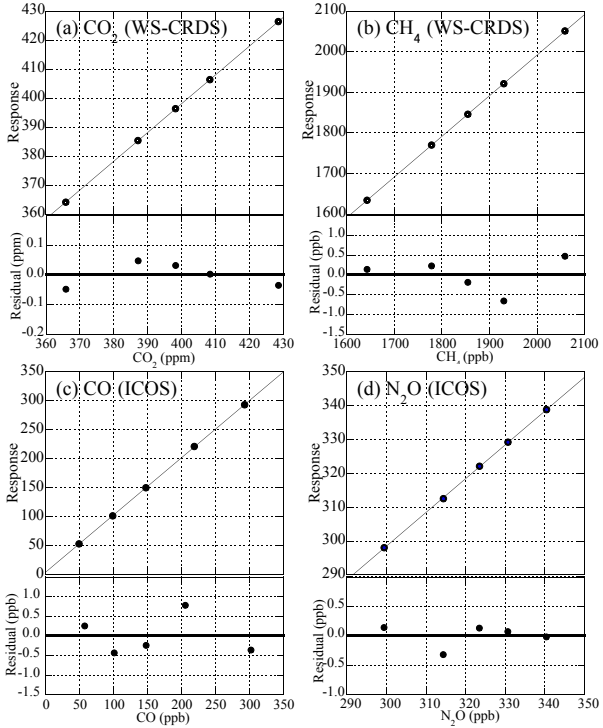

Fig. 4. Plots of the analyzer response versus assigned concentrations of 5 working standard gases for CO_2 **(a)** and CH_4 **(b)** of the WS-CRDS analyzer, and CO **(c)** and N_2O **(d)** of the ICOS analyzer. The solid line represents a linear least squares fit to all the data points. Residuals of the fit are plotted in the lower panels.

AMTD
5, 7067–7094, 2012

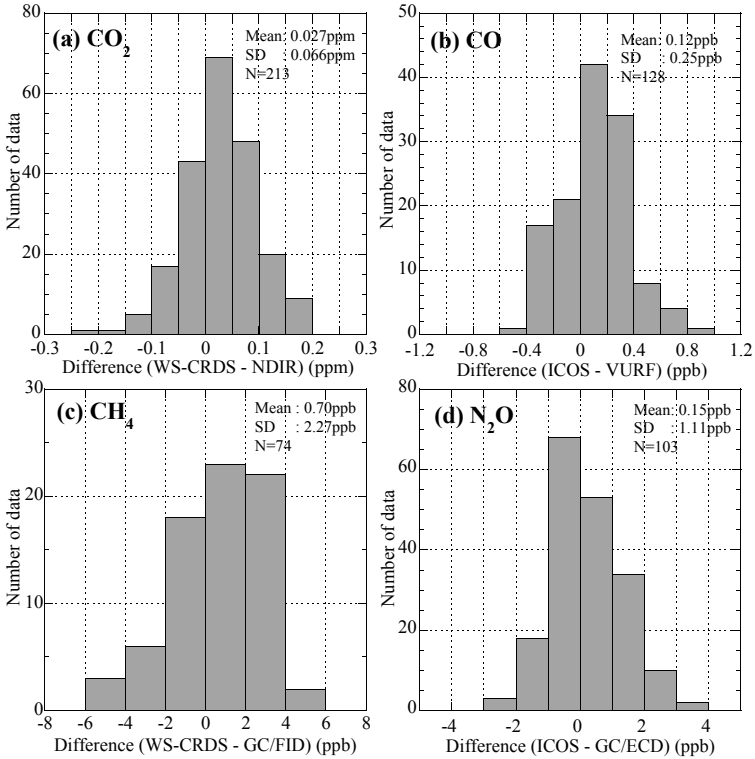

Fig. 5. Frequency distributions of the differences in air sample measurements for CO_2 between the WS-CRDS and the NDIR analyzers **(a)**, CO between the ICOS and the VURF analyzers **(b)**, CH_4 between the WS-CRDS and the GC/FID analyzers **(c)**, and N_2O between the ICOS and the GC/ECD analyzers **(d)**.

AMTD
5, 7067–7094, 2012